A first-in-class multimodal immunotherapy for induction of tertiary lymphoid structures as a novel therapeutic strategy for solid tumors

LB263

Anne R. Diers [1], Qiuchen Guo [1], John D. Christie [1], David Krisky [1], Fabrina M. Gaspal [2], Erin Richardson [2], Charlotte G. Smith [3], David R. Withers [2], Adam P. Croft [3], Paul P. Tak [1], Francesca Barone [1]
[1] Candel Therapeutics, Needham, MA, USA; [2] Institute of Immunology and Immunotherapy, College of Medical and Dental Sciences, University of Birmingham, Birmingham, UK;
[3] Rheumatology Research Group, Institute of Inflammation and Ageing, University of Birmingham, Birmingham, UK

Tertiary lymphoid structures (TLS) in cancer immunotherapy

Scheme of TLS formation and maturation [1]

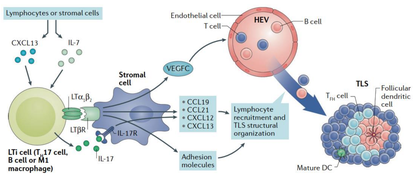

- The formation of organized intratumoral lymphocyte aggregates or **tertiary lymphoid structures (TLS)** has been associated with response to ICI, suggesting that therapeutics able to induce intratumoral TLS could enhance the response in ICI nonresponsive tumors.
- TLS assembly in the tissue requires a series of events, including antigen presentation, stromal cell activation, and immune cell activation/aggregation, which are difficult to obtain with a single therapeutic.

The enLIGHTEN™ Discovery Platform

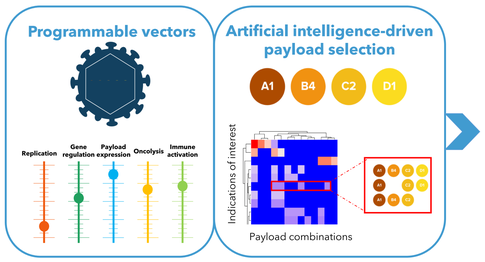

- enLIGHTEN™ enables the generation of multimodal agents able to overcome barriers in the tumor microenvironment and improve response in immunotherapy resistant patients.
- Vectors are generated with programmable features engineered through the combinations of vector genome deletion/disruption and insertion of synthetic, non-native encodable elements.
- In silico predicted payload combinations are encoded in single gene minivectors and tested in in vitro and in vivo assays.

Development of TLS inducing vector using the enLIGHTEN™ Discovery Platform. The enLIGHTEN™ advanced analytics platform was applied to ICI-treated patient datasets [2-7], and the predicted payload components included factors regulating the development of TLS. The top two scoring combinations **(Multiplex A and Multiplex B)** were tested for effects on TLS induction and anti-tumor efficacy.

Alpha-201: an ideal programmable vector for use in combination with ICI

Alpha-201, a replication-defective oncolytic herpes simplex virus, was selected from a suite of programmable vectors due to its ability to release tumor antigens and activate pathways associated with response to ICI (Fig. 1). A library of single gene encoding Alpha-201 vectors was constructed, each expressing one in silico predicted payload component, and validated for its payload production and oncolytic activity (Fig. 2).

Figure 1

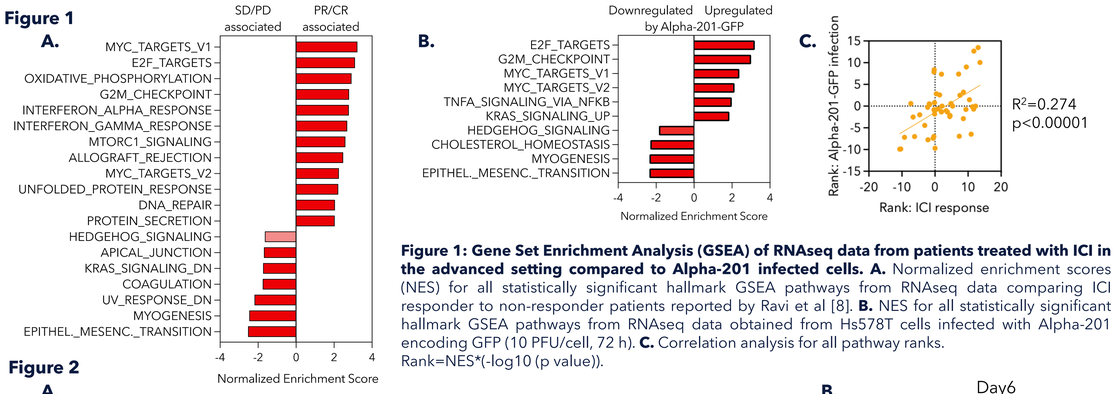

Figure 1: Gene Set Enrichment Analysis (GSEA) of RNAseq data from patients treated with ICI in the advanced setting compared to Alpha-201 infected cells. A. Normalized enrichment scores (NES) for all statistically significant hallmark GSEA pathways from RNAseq data comparing ICI responder to non-responder patients reported by Ravi et al [8]. **B.** NES for all statistically significant hallmark GSEA pathways from RNAseq data obtained from Hs578T cells infected with Alpha-201 encoding GFP (10 PFU/cell, 72 h). **C.** Correlation analysis for all pathway ranks. Rank=NES*(-log10 (p value)).

Figure 2

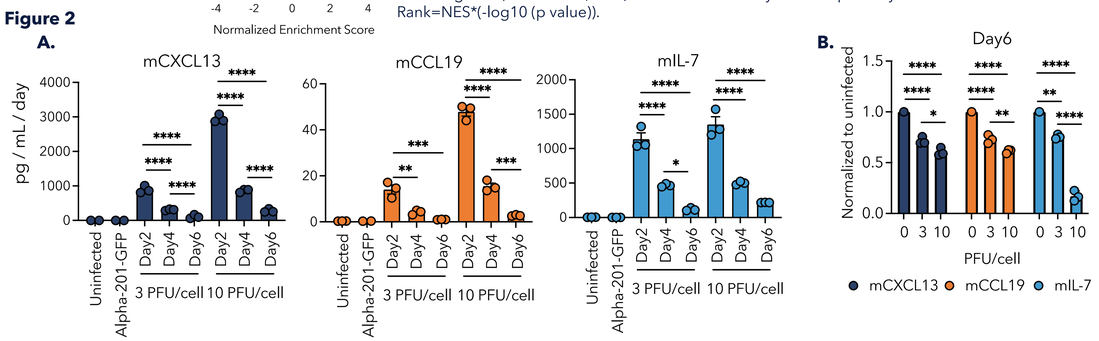

Figure 2: Validation of minivectors. A. Hs578T cells were infected with Alpha-201 vectors (3 or 10 PFU/cell), and then conditioned medium was collected every 2 days for quantification of payload production rates. **B.** Cell viability was measured with RealTime-Glo™ 6 days after infection. ANOVA with Tukey's correction, *p<0.05, **p<0.01, ***p<0.001, ****p<0.0001.

TLS induction by programmable vector-mediated delivery of in silico predicted payload combinations

The ability of minivector combinations to induce TLS was tested in murine salivary glands, a tissue highly permissive to TLS formation. Alone, Alpha-201-GFP infection enhanced immune infiltration into infected glands (Fig. 3). The delivery of a combination of minivectors, encoding in silico predicted payloads, was able to induce TLS that were increased in number, size, and organization as compared to control vector (Fig. 4). Induced TLS also yield mature fibroblastic reticular cell networks and de novo expression of CCL21 (Fig. 5).

Figure 3

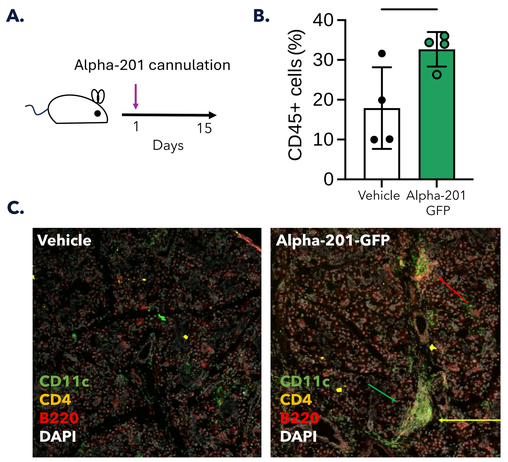

Figure 3: Murine salivary gland model of TLS induction.
A. Minivector combinations (total dose = $3x10^7$ PFU) were administered via cannulation of the submandibular glands of anesthetized mice, and glands were harvested for histologic and flow cytometric analysis 15 days later. **B.** Flow cytometry analysis of $CD45^+$ cells. **C.** Immunofluorescent images from salivary glands after administration of vehicle or Alpha-201-GFP. Dendritic cells (CD11c, green), $CD4^+$ T cells (CD4, yellow), B cells (B220, red), and nuclei (DAPI, white) are visualized. * $p < 0.05$. 10X magnification.

Figure 4

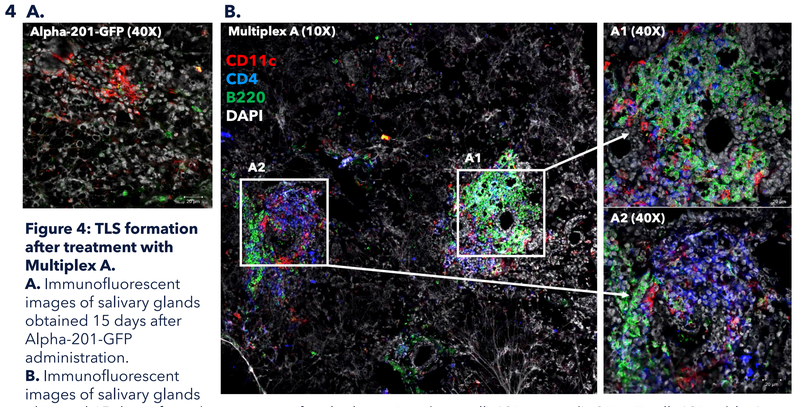

Figure 4: TLS formation after treatment with Multiplex A.
A. Immunofluorescent images of salivary glands obtained 15 days after Alpha-201-GFP administration.
B. Immunofluorescent images of salivary glands obtained 15 days after administration of Multiplex A. Dendritic cells (CD11c, red), $CD4^+$ T cells (CD4, blue), B cells (B220, green), and nuclei (DAPI, white) are visualized.

Figure 5

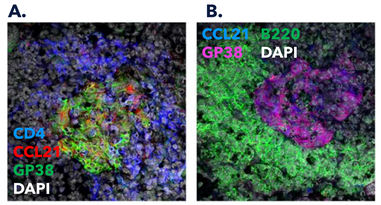

Figure 5: Mature fibroblastic reticular cell network and de novo CCL21 expression in TLS induced by Multiplex A.
Immunofluorescent images of salivary glands 15 days after administration of Multiplex A. **A.** CCL21 (red) and fibroblastic reticular cells (GP38, green) are colocalized with $CD4^+$ T cells (CD4, blue). **B.** CCL21 (blue) and GP38 (purple) are colocalized with B cells (B220, green). Nuclei (DAPI, white). 40X magnification.

Robust in vivo anti-tumor efficacy upon delivery of factors regulating TLS induction

The anti-tumor efficacy of combinations of minivectors encoding in silico predicted payloads was tested in EMT6 tumor-bearing mice. Both Multiplex A and Multiplex B induced tumor growth inhibition compared to vehicle control mice (Fig. 6). In a survival study, the combination of anti-PD-1 antibody therapy and multiplex treatment increased the number of long-term survivors (>40 days) as compared to controls (Fig. 7).

Figure 6

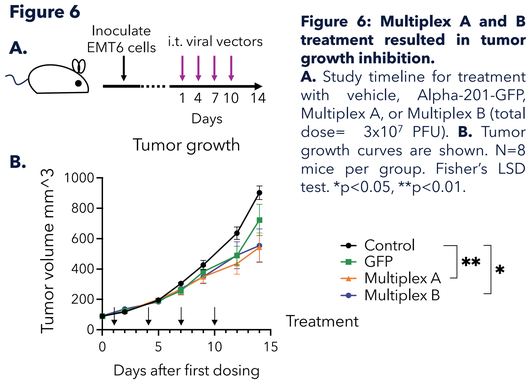

Figure 6: Multiplex A and B treatment resulted in tumor growth inhibition.
A. Study timeline for treatment with vehicle, Alpha-201-GFP, Multiplex A, or Multiplex B (total dose= $3x10^7$ PFU). **B.** Tumor growth curves are shown. N=8 mice per group. Fisher's LSD test. *p<0.05, **p<0.01.

Figure 7

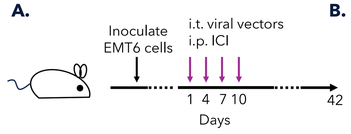

B. Number of long-term survivors

	Vehicle	Multiplex A	Multiplex B
+ IgG isotype control	0/8	0/6	0/6
+ anti-PD-1 Ab	0/6	1/6	1/7

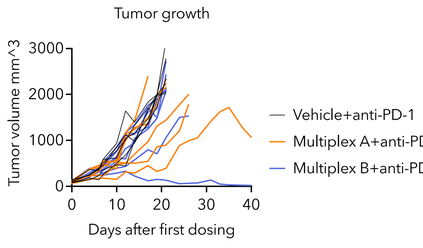

Figure 7: Combined multiplex and ICI treatment increased the number of long-term survivors.
A. Study timeline for treatment with vehicle, Alpha-201-GFP, Multiplex A, or Multiplex B (total dose = $3x10^7$ PFU) with and without anti-PD-1 (clone: RMP1-14) or isotype control antibodies (IgG, 10mg/kg).
B. Long-term survivors for each group and tumor growth curves for groups with anti-PD-1 treatment. N=6-8 mice per group.

Conclusions

- Here we present data on two new experimental agents that induce TLS in a permissive tissue and have robust anti-tumor activity in a model of breast cancer through a combination of vector- and payload-dependent effects.
- Combination of Alpha-201 multiplexes with anti-PD-1 therapy increased the number of long-term survivors.
- Together, these data demonstrate the ability of enLIGHTEN™ to design multimodal specific therapeutics resulting in the development of a first-in-class immunotherapeutic for TLS induction and anti-tumor activity in solid tumors.

References:
1. Sautès-Fridman C. et al. Nat Rev Cancer 2019; 19(6):307325.
2. Gide T.N. et al. Cancer Cell 2019; 35(2):238-255.e6.
3. Hugo W. et al. Cell 2016;165(1):35-44.
4. Liu D. et al. Nat Med 2019;25(12):1916-1927.
5. Riaz N. et al. Cell 2017;171(4):934-949.e16.
6. Van Allen E.M. et al. Science 2015;350(6257):207-211.
7. McDermott D.F. et al. Nat Med 2018. 24(6):749–757.
8. Ravi A. et al. Nat Genet 2023;55(5):807-819.

Contact email: info@candeltx.com